Supporting Information

20.0% Efficiency of Ternary Organic Solar Cells Enabled by A Novel Wide Band Gap Polymer Guest Donor

Junkang Zhou,[a,l] Xinjie Zhou,[b,l] Hongge Jia,[c,*] Lijun Tu,[a] Siqi Wu,[a] Xiaomin Xia,[a] Xin Song[b,*] and Yongqiang Shi[a,*]

[a] Key Laboratory of Functional Molecular Solids, Ministry of Education, and Anhui Key Laboratory of Molecule-Based Materials and Anhui Key Laboratory of Biomedical Materials and Chemical Measurement. School of Chemistry and Materials Science, Anhui Normal University, Anhui, 241002, China.
Email: shiyq@ahnu.edu.cn
[b] School of Materials Science and Engineering, Jiangsu Engineering Laboratory of Light-Electricity-Heat Energy-Converting Materials and Applications, Changzhou University, Changzhou 213164, China.
Email: xin.song@cczu.edu.cn
[c] College of Materials Science and Engineering, Heilongjiang Provinces Key Laboratory of Polymeric Composite Materials, Qiqihar University, Qiqihar, 161006, China.
Email: Jiahongge@qqhru.edu.cn
[l] Contributed equally to this work.

1. Materials and Methods.

All commercially available solvents, reagents, and chemicals were used as received without further purification unless otherwise stated. Anhydrous toluene was distilled from Na/benzophenone, and anhydrous triethylamine and acetonitrile were distilled from CaH_2 under argon. Unless otherwise stated, all operations and reactions were carried out under argon using standard Schlenk line techniques. ^1H and ^{13}C NMR spectra were recorded on a Bruker Ascend 400 and 500 MHz spectrometer, and the chemical shifts were referenced to residual protio-solvent signals. Differential scanning calorimetry (DSC) curves were recorded on Mettler STAR^e (TA Instrument) in nitrogen with a heating ramp of 10 ºC min^{-1}, and thermogravimetric analysis (TGA) curves were collected on Mettler STAR^e (TA Instrument). UV-vis absorption spectra were

measured using a Shimadzu UV-2500 recording spectrophotometer. PM6, BTP-eC9 were purchased from Volt-Amp Optoelectronics Tech. Co., Ltd, Dongguan, China. Ethanol, chlorobenzene and 1-chloronaphthalene were purchased from Aladdin Inc. All materials were used without further purification. ITO substrates were purchased from Advanced Election Technology Co., Ltd. PNDI-FN-Br were purchased from Nanjing Zhiyan Inc.

2. Materials Synthesis.

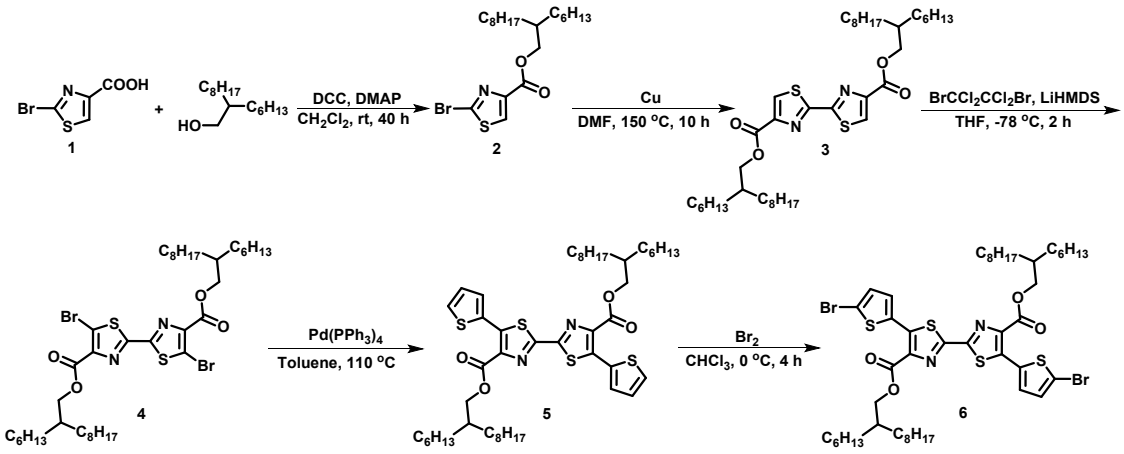

Scheme S1. The synthetic route to monomer (6).

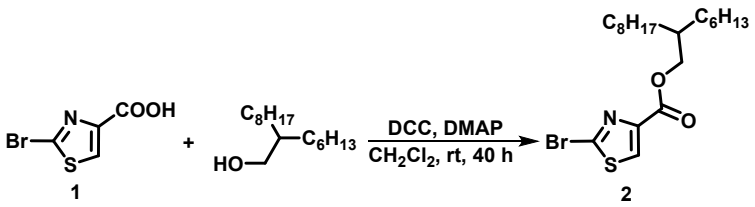

To the mixture of 2-bromothiazole-4-carboxylic acid 1 (2.75 g, 13.2 mmol), DCC (3.2 g, 15.8 mmol), and DMAP (0.57 g, 4.6 mmol) in a 100 mL round-bottom flask with 60 mL of CH_2Cl_2 were added 2-hexyldecan-1-ol (6.4 g, 26.4 mmol). The mixture was stirred for 40 h under the Ar_2 atmosphere, was poured into 30 mL of water, and then extracted with CH_2Cl_2 and then dried over anhydrous $MgSO_4$. After filtration, the reaction mixture was concentrated under a reduced pressure, and the residue was purified by flash column chromatography using petroleum ether/CH_2Cl_2 (3:1) as the eluent to give 2-hexyldecyl 2-bromothiazole-4-

carboxylate 2 (4.1 g, 82%). ^{1}H NMR (400 MHz, Chloroform-*d*) δ 8.08 (s, 1H), 4.27 (d, *J* = 6.0 Hz, 2H), 1.81 (q, *J* = 5.8 Hz, 1H), 1.32 (d, *J* = 30.6 Hz, 27H), 0.89 (t, *J* = 6.7 Hz, 7H).^{13}C NMR (CDCl3, 100 MHz) δ (ppm): δ160.72, 147.39, 136.82, 130.53, 68.72, 65.76, 40.54, 37.34, 31.91, 31.89, 31.82, 31.24, 29.76, 29.96, 29.36, 29.32, 26.90, 26.87, 26.68, 26.65.

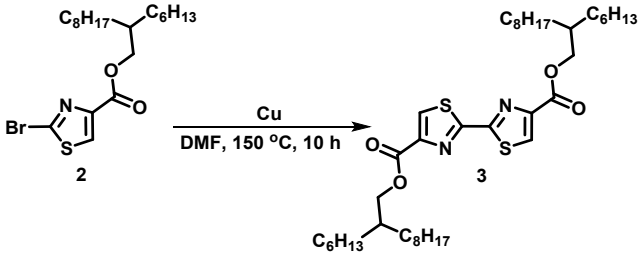

To a solution of 2 (1 g, 2.76 mmol) in 30 mL of dimethylformamide (DMF), Cu (0.4 g, 8.28 mmol, 3 equiv) was added in one portion under nitrogen. The reaction mixture was heated at 150 °C for 12 h. Then, the solvent was removed under reduced pressure, and the residue was purified by column chromatography on silica gel with petroleum ether/ethyl acetate (5:1) as the eluent to give product 3 as a transparent liquid (0.7 g, 70%).^{1}H NMR (400 MHz, Chloroform-*d*) δ 8.25 (s, 2H), 4.30 (d, *J* = 5.8 Hz, 4H), 1.82 (s, 2H), 1.29 (d, *J* = 11.1 Hz, 46H), 0.91 – 0.87 (m, 15H). ^{13}C NMR (CDCl3, 100 MHz) δ (ppm): δ161.04, 160.89, 148.17, 129.33, 68.52, 65.55, 40.53, 37.39, 31.92, 31.90, 31.82, 31.37, 30.93, 29.96, 29.76, 29.63, 29.57, 29.36, 29.93, 22.69, 14.11.

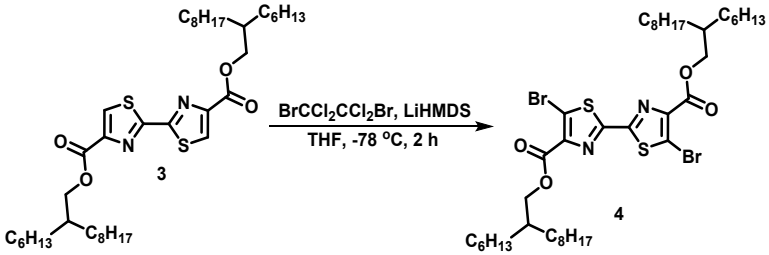

Compound 3 (3 g, 6.74 mmol) and $BrCCl_2CCl_2Br$ (4.38 g, 13.48 mmol) were dissolved in anhydrous tetrahydrofuran (THF). Lithium hexamethyldisilazide (LiHMDS) (14.83 mL, 14.83 mmol) was added slowly at −78 °C and stirred for 20 min under N_2. Then, to the reaction mixture was added saturated NH_4Cl aqueous solution. The aqueous phase was extracted with dichloromethane three times, the combined

organic phase was evaporated under reduced pressure, and the residue was purified by column chromatography using petroleum ether/ethyl acetate (5:1) as the eluent to afford the product compound 4 (yield: 90%).[1]H NMR (400 MHz, Chloroform-*d*) δ 4.33 (d, *J* = 5.7 Hz, 4H), 1.82 (s, 1H), 1.30 (d, *J* = 11.7 Hz, 50H), 0.90 (dt, *J* = 6.9, 3.2 Hz, 14H). [13]C NMR (101 MHz, Chloroform-*d*) δ 161.14, 160.98, 148.29, 129.42, 68.65, 37.50, 32.02, 31.93, 31.48, 30.07, 29.73, 29.68, 29.43, 26.86, 26.83, 22.79, 14.23.

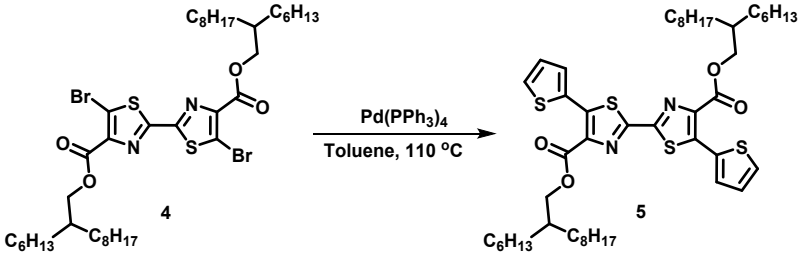

100 mL round-bottom flask was added 4 (1.0 g, 1.33 mmol), 2-(tributylstannyl)thiophene (1.01 g, 3.33 mmol), $Pd(PPh_3)_4$ (70 mg, 0.06 mmol), and toluene (10 mL). The reaction flask was purged with argon and sealed, and the reaction mixture was heated at 120 °C for 11 h. After cooling to room temperature, the reaction solution was poured into 100 mL H_2O and extracted with 100 mL CH_2Cl_2 3 times. The combined organic layer was dried over $MgSO_4$, and the solvent was evaporated under reduced pressure. The crude product was purified by column chromatography on silica gel using petroleum ether/ethyl acetate (3:1) as the eluent to give compound 5 as a chartreuse solid (yield: 52%).[1]H NMR (400 MHz, Chloroform-*d*) δ 7.54 – 7.49 (m, 3H), 7.12 (dd, *J* = 5.1, 3.7 Hz, 1H), 4.25 (d, *J* = 6.0 Hz, 3H), 1.75 (s, 2H), 1.27 (d, *J* = 12.0 Hz, 48H), 0.91 – 0.82 (m, 12H).[13]C NMR (101 MHz, Chloroform-*d*) δ 162.15, 157.21, 141.08, 131.03, 130.21, 129.44, 127.64, 68.81, 37.28, 31.92, 31.84, 31.24, 30.00, 29.65, 29.60, 29.38, 26.71, 26.67, 14.14.

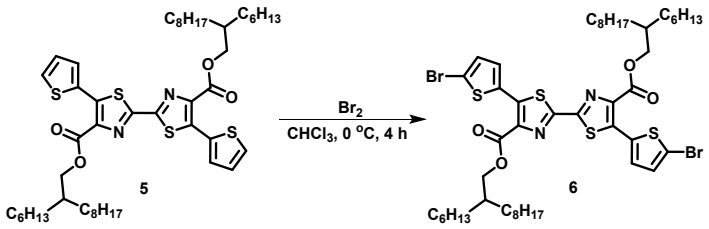

Br_2 (876 mg, 5.5 mmol) was added to a solution of 5 (1.2 g, 1.37 mmol) in $CHCl_3$ 10 mL in one portion. The reaction mixture was stirred at 0 °C for 4 h, and 30 mL H_2O

was then added. Next, the reaction mixture was extracted with 30 mL CH_2Cl_2 for 3 times, and the combined organic layer was washed with 50 mL brine and then dried over anhydrous $MgSO_4$. After filtration, the solvent was removed under reduced pressure to afford a chartreuse liquid, which was purified by column chromatography over silica gel with petroleum ether/ethyl acetate (3:1) as the eluent. The compound 6 was obtained as green solid (yield: 80%). ^{1}H NMR (400 MHz, Chloroform-*d*) δ 4.28 (d, *J* = 6.0 Hz, 1H), 1.77 (s, 2H), 1.29 (d, *J* = 19.6 Hz, 42H), 0.88 (dt, *J* = 6.9, 3.5 Hz, 13H).^{13}C NMR (101 MHz, Chloroform-*d*) δ 162.03, 156.86, 140.90, 131.64, 131.33, 130.28, 117.54, 69.02, 37.29, 31.94, 31.86, 31.28, 30.02, 29.68, 29.62, 29.40, 26.73, 26.70, 22.72. HRMS: m/z (ESI) calculated for ($C_{48}H_{70}Br_2N_2O_4S_4$): 1026.26, $[M+H]^+$found: 1027.26273.

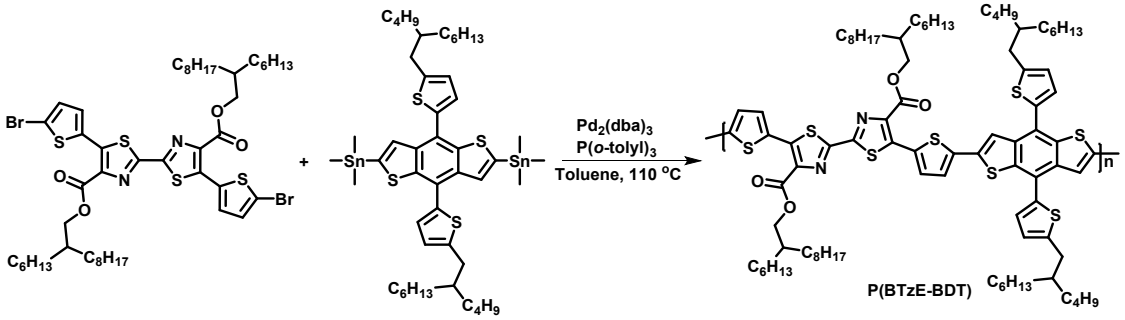

A glass tube was charged with the two monomers (0.1 mmol each), tris(dibenzylideneacetone)dipalladium (0) ($Pd_2(dba)_3$), and tris(o-tolyl) phosphine ($P(o\text{-tolyl})_3$) (1:8, $Pd_2(dba)_3$:$P(o\text{-tolyl})_3$ molar ratio; Pd loading: 0.03-0.05 equiv). The tube and its contents were subjected to 3 pump/purge cycles with argon, followed by the addition of 2.5 mL anhydrous toluene via syringe. The tube was sealed under argon flow and then stirred at 120 ºC for 72 h. Then, 50 μL 2-(tributylstanny) thiophene was added and the reaction mixture was stirred at 120 ºC for 0.5 h. Finally, 50 μL 2-bromothiophene was added and the reaction mixture was stirred at 120 ºC for another 0.5 h. After cooling to room temperature, the reaction mixture was slowly dripped into 100 mL methanol (containing 0.5 mL 12 N hydrochloric acid) under vigorous stirring. After stirring for 1 h, the solid precipitate was transferred to a Soxhlet thimble. After drying, the crude product was subjected to sequential Soxhlet extraction with the

solvent sequence of methanol, acetone, hexane, dichloromethane, and chloroform. The chloroform fraction was concentrated by removing most of solvent under reduced pressure and then precipitated into methanol. The solid was collected by filtration and dried in vacuum to afford the polymer as a deep colored solid

3. NMR Spectra of Monomer and Polymer

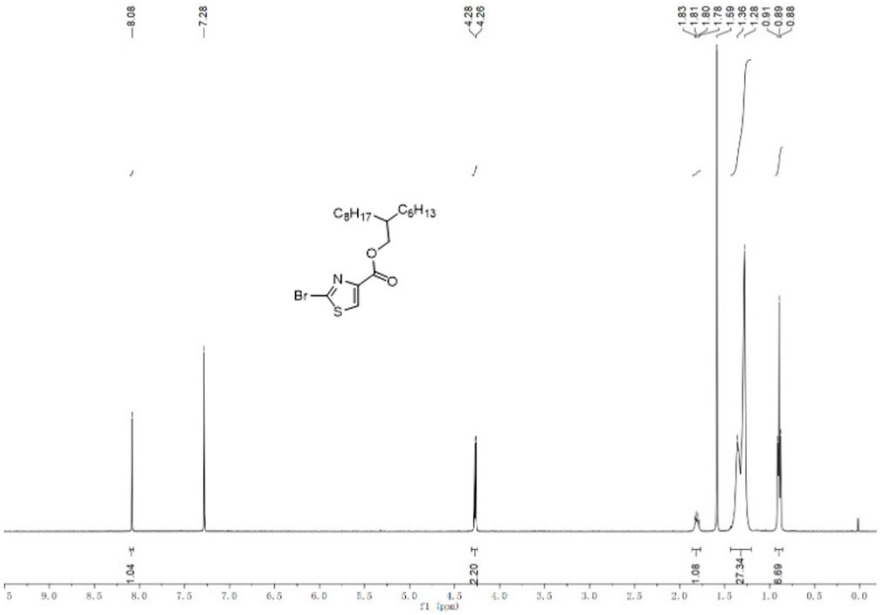

Figure S1. ^{1}H NMR spectrum of monomer **2** (400 M, r.t., in $CDCl_3$).

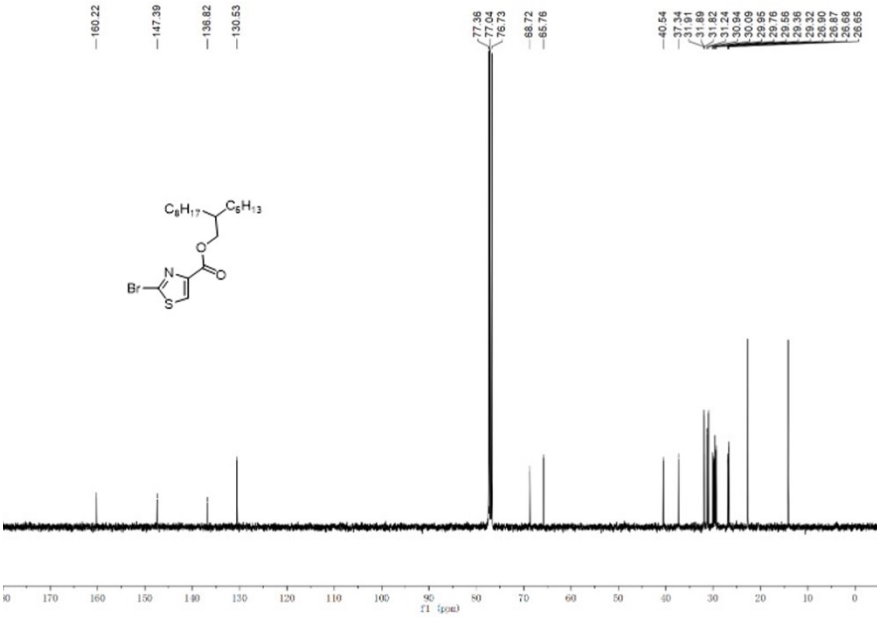

Figure S2. ^{13}C NMR spectrum of compound 2 (100 M, r.t., in $CDCl_3$).

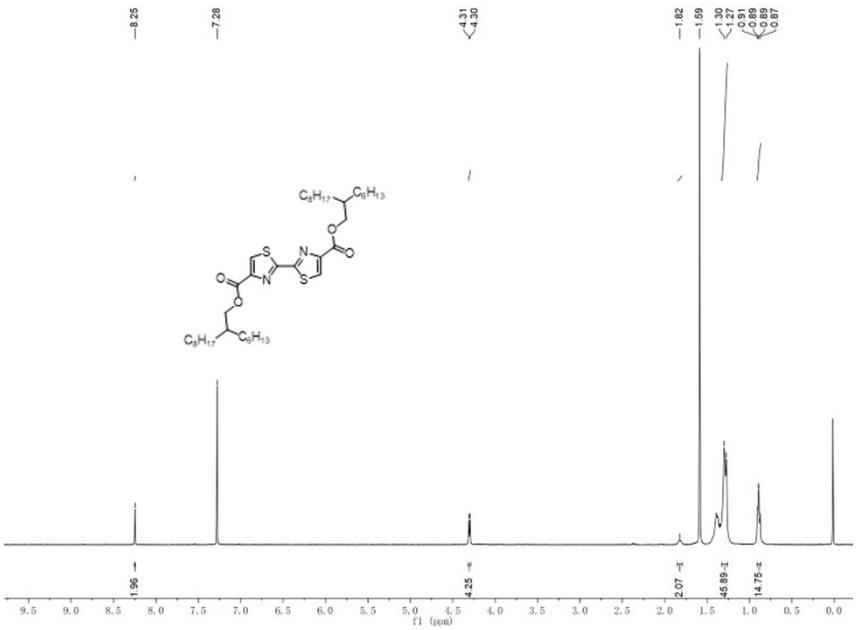

Figure S3. ^{1}H NMR spectrum of monomer **3** (400 M, r.t., in $CDCl_3$).

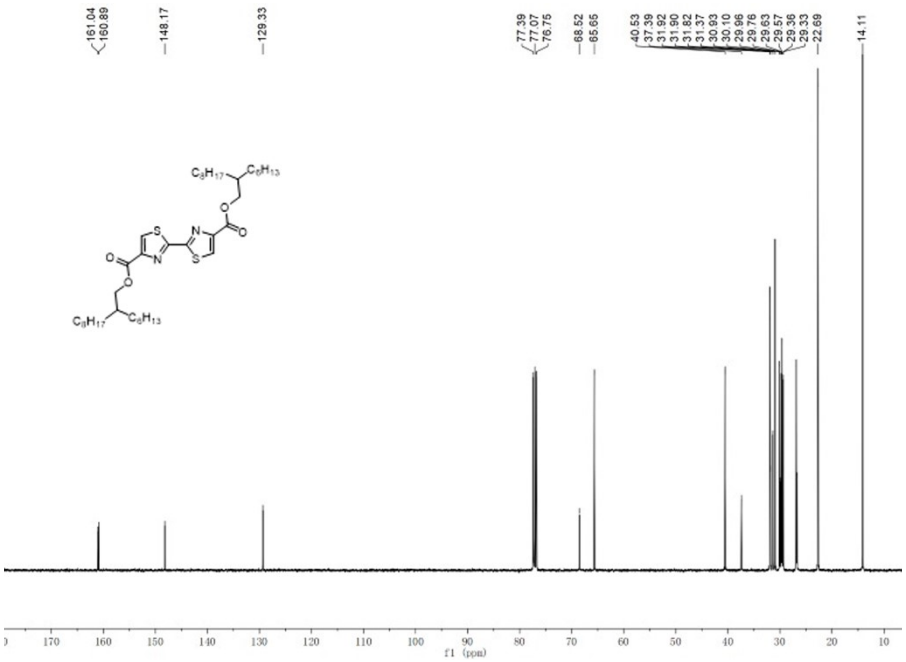

Figure S4. ^{13}C NMR spectrum of compound **3** (100 M, r.t., in $CDCl_3$).

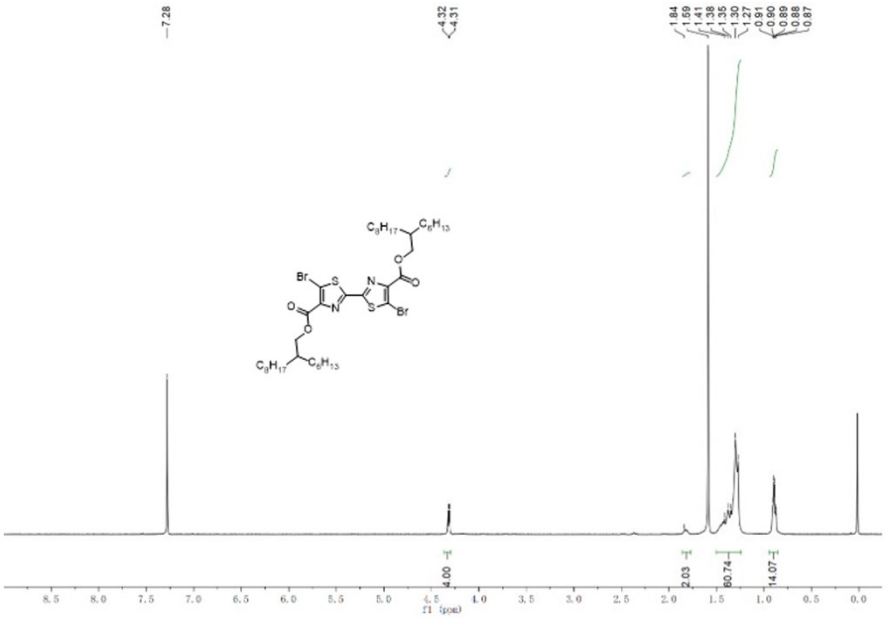

Figure S5. ^{1}H NMR spectrum of monomer **4** (400 M, r.t., in $CDCl_3$).

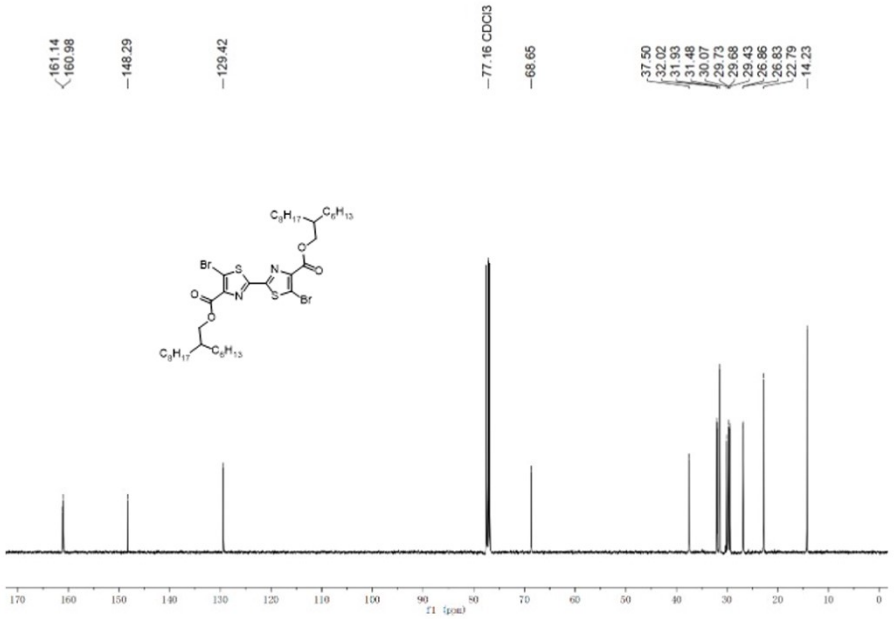

Figure S6. ^{13}C NMR spectrum of compound **4** (100 M, r.t., in $CDCl_3$).

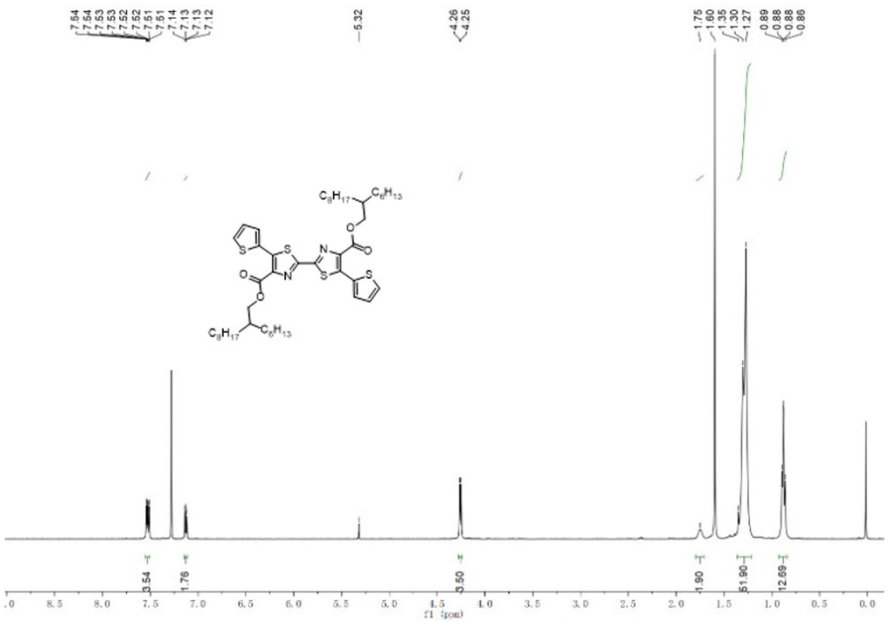

Figure S7. ^{1}H NMR spectrum of monomer **5** (400 M, r.t., in $CDCl_3$).

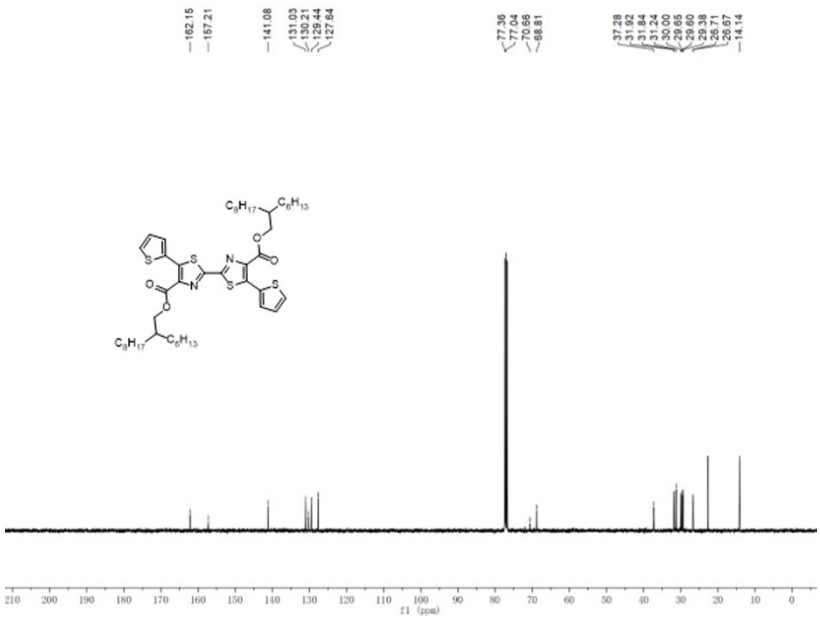

Figure S8. ^{13}C NMR spectrum of compound **5** (100 M, r.t., in $CDCl_3$).

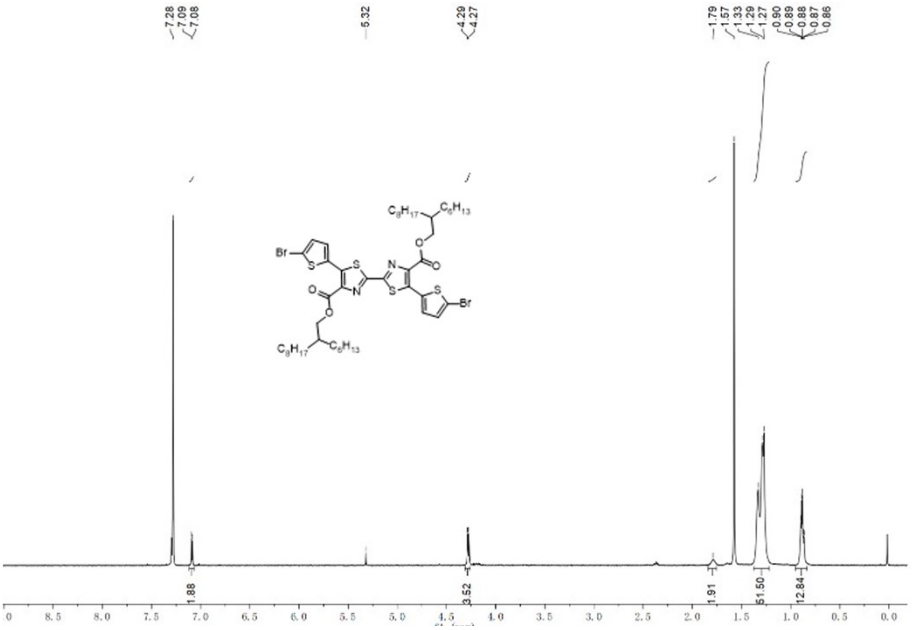

Figure S9. ^{1}H NMR spectrum of monomer **6** (400 M, r.t., in $CDCl_3$).

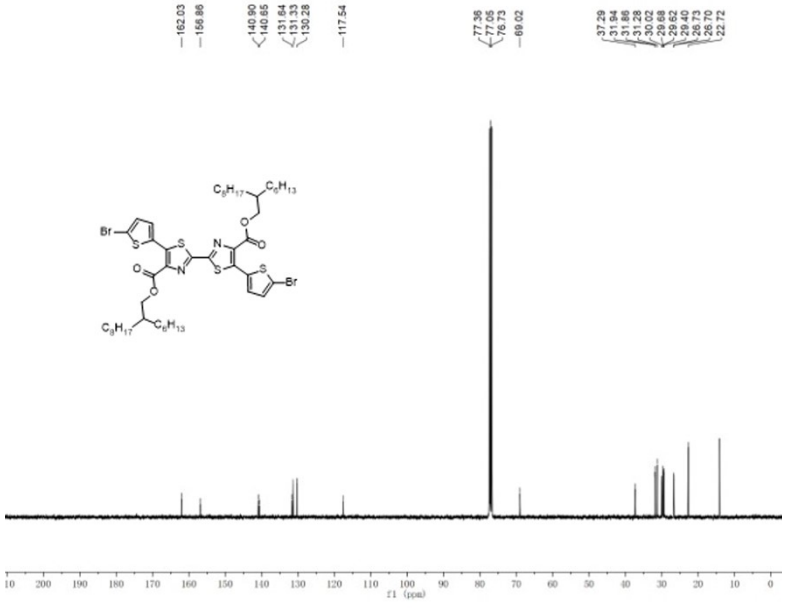

Figure S10. ^{13}C NMR spectrum of compound **6** (100 M, r.t., in $CDCl_3$).

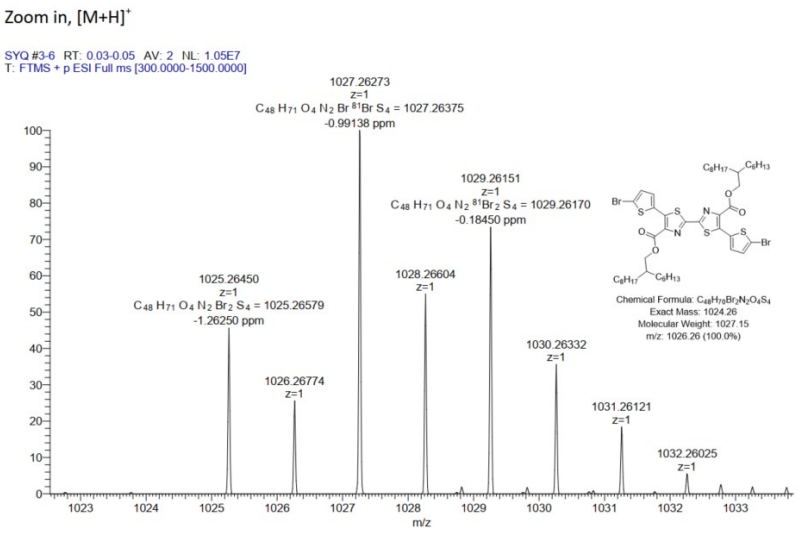

Figure S11. HRMS of BTzE monomer (6).

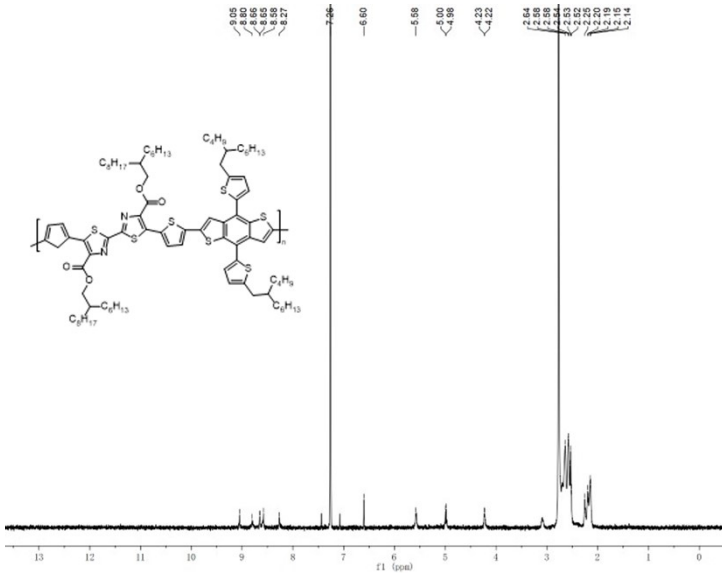

Figure S12. ^{1}H NMR spectrum of polymer P(BTzE-BDT) (500M, 80 ℃, in $C_2D_2Cl_4$).

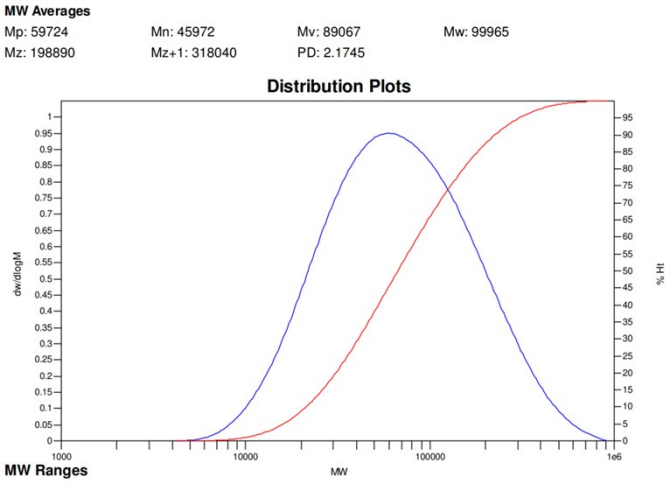

Figure S13. GPC curve of polymer P(BTzE-BDT) measure at 150 °C using 1,2,4-trichlorobenzene as the eluent.

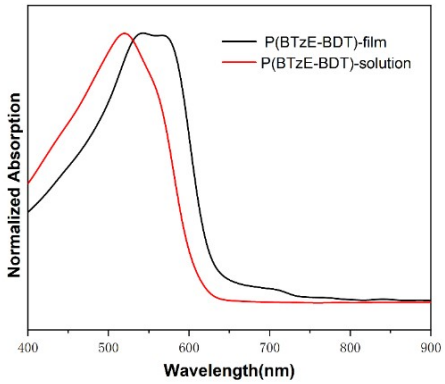

Figure S14.Nornailized UV-vis absorbance spectra of the polymer in chloroform solution and as thin films.

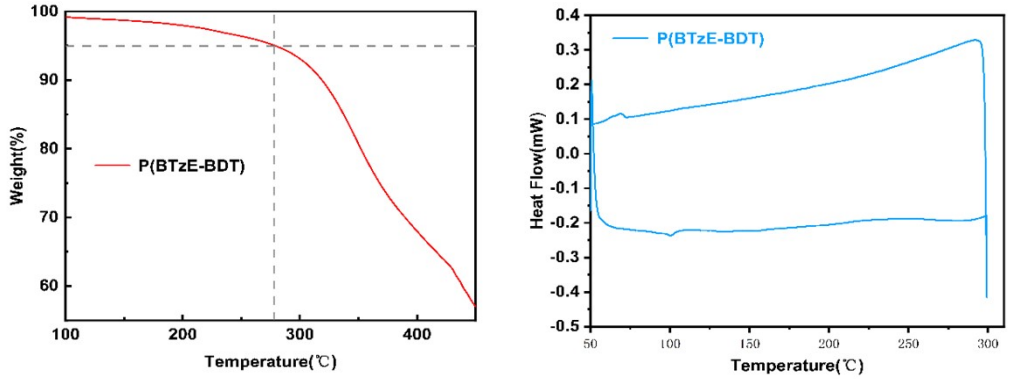

Figure S15. (a)Thermogravimetric analysis and of P(BTzE-BDT) at a heating rate of 10 ºC min^{-1}. (b) DSC thermograms of polymer P(BTzE-BDT). The DSC curves are from the second heating and first cooling scans with a ramp rate of 10 ºC min^{-1}. N_2 was used as the purge gas for both TGA and DSC measurements.

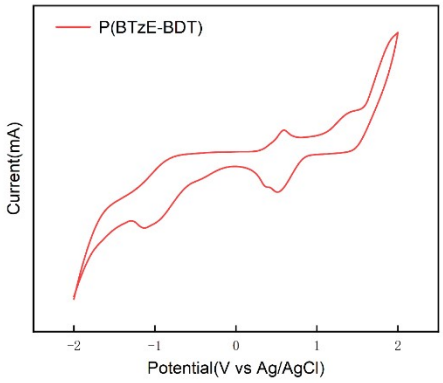

Figure S16.Cyclic voltammograms of P(BTzE-BDT) measured in 0.1 M tetrabutylammonium hexafluorophosphate acetonitrile solution with the Fc/Fc^{+} redox couple as an external standard at a scanning rate of 0.05 V s^{-1}.

Table S1 Photovoltaic parameters for two acceptors-based OSCs in literature.

Ternary system	*Jsc*[mA cm^{-2}]	FF[%]	*Voc*[V]	PCE(%)	Ref.
PM6:IDIC:TOBDT	21	70	0.91	14	1
PM6:L8-BO:BTP-ThMe	25.9	77.7	0.88	17.7	2
PM6:L8-BO:BTP-ThMeCl	26.7	82.2	0.87	19.1	2
PM6:L8-BO:DY-TF	26.93	78.5	0.905	19.13	3
D18:N3:DOY-C4	28.07	79.4	0.853	19.01	4
D18:N3:DP-BTP	27.95	78.5	0.87	19.07	5

Table S2 Photovoltaic parameters for two donors-based OSCs in literature and this study.

D1: D2: A	*V*oc (V)	*Jsc* (mA cm^{-2}))	FF (%)	PCE (%)	Ref.
PM6:J71:Y6	0.850	25.55	76.0	16.5	6
PBDT-ST:PNDT-ST:Y6-T	0.909	24.04	75.9	16.57	7
PM6:PDHP-Th:Y6	0.850	26.60	71.7	16.8	8
PM6:TPD-3F:Y6	0.88	25.60	73.4	17.0	9
PM6:PBB1-Cl:Y6-BO-4Cl	0.866	26.84	74.63	17.36	10
PM6:S3:Y6	0.856	25.86	79.17	17.53	11
PM6:5BDTBDD:BTP-BO-4Cl	0.843	26.83	77.43	17.54	12
D18:ZW1:Y6	0.860	27.97	76.82	17.61	13
PTQ10:PTVT-T:m-BTP-PhC6	0.883	27.02	80.1	19.11	14
PM6:D18:L8-BO	0.896	26.70	81.9	19.6	15
PM6:PBB-Cl:BTP-eC9	0.853	28.53	78.23	19.04	16
PM6:PhIsSe:Y6	0.845	25.70	75.5	16.4	17
PM6:P(BTzE-BDT):BTP-eC9	0.870	28.30	81.2	20.0	**This work**

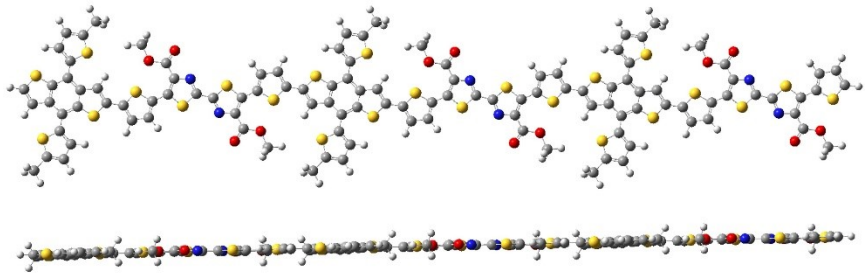

Figure S17. Calculated molecular orbitals of trimers of P(BTzE-BDT) at the (B3LYP/6-31G(d,p)) level. The alkyl chains are replaced with methyl chains for computational simplicity.

4. Device Fabrication and Characterization

The devices were fabricated with conventional structures of ITO/HTL/BHJ/PNDI-F3N-Br/Ag (100 nm). The patterned ITO glass substrates were cleaned sequentially under sonication with deionized water and isopropanol, and then dried at 60 ℃ in a baking oven overnight. After UV-ozone treatment for 15 min, the PEDOT:PSS was deposited on ITO substrates at 4500 rpm for 30 s, and then baked in air at 150 °C for 10 min; Sequentially, the active layer solution of PM6:BTP-eC9 or PM6: P(BTzE-BDT):BTP-eC9 (1:1 , 20 mg/ml) was spin-coated at 3000 rpm for 30 s, and then baked in air at 100 °C for 10 min. After that, PNDI-F3N-Br solution with a concentration of 0.5 mg mL^{-1} was spin-coated on the active layer at 3000 rpm for 30 s. To complete the fabrication of the devices, 100 nm of Ag was thermally evaporated through a mask under a vacuum of ~5×10^{-4} mbar. The active area of the devices was 0.06 cm^2.

J-V and EQE measurement

The photovoltaic performance was measured under an AM 1.5G spectrum from a solar simulator (Newport). The current density-voltage (*J-V*) characteristics were recorded with a Keithley 2400 source meter. The light intensity of light source was calibrated before the testing by using a standard silicon solar cell, as calibrated by a National Renewable Energy Laboratory (NREL) certified silicon photodiode, giving a value of 100 mW/cm^2 in the test. The external quantum efficiency (EQE) spectra were obtained on a commercial EQE measurement system (Taiwan, Enlitech, QE-R3011). The light intensity at each wavelength was calibrated by a standard single-crystal Si photovoltaic cell.

Atomic Force Microscopy

The as-prepared samples were subsequently sent out for the AFM and c-AFM measurements using the Cypher ES Oxford Instruments at a bias of 500 mV.

UV-vis Absorption Measurement

UV-vis absorption spectra were recorded on a Shimadzu spectrophotometer.

Transient optoelectronic characterizations

In the Photo-CELIV, TPC and TPV measurements, the OSCs were fabricated with the same method as mentioned above. The data were obtained by the all-in-one characterization platform, Paios (Fluxim AG, Switzerland).

Table S3. Photovoltaic parameters of the PM6:P(BTzE-BDT):BTP-eC9 device with different P(BTzE-BDT) content

PM6: P(BTzE-BDT):BTP-eC9 (D1:D2:A)	V_{OC} (V)	J_{SC} (mA cm^{-2})	FF (%)	PCE (%)
1:0:1	0.87	27.6	78.0	18.8
0.95:0.05:1	0.87	28.3	81.2	20.0
0.8:0.2:1	0.87	27.0	75.6	17.8
0:1:1	0.86	21.6	62.9	11.7

Table S4 Photovoltaic parameters of PM6:P(BTzE-BDT):BTP-eC9 device with different thermal annealing temperature.

Annealling Temperature (^{o}C)	V_{OC} (V)	J_{SC} (mA cm^{-2})	FF (%)	PCE (%)
80	0.87	28	80.4	19.6
100	0.87	28.3	81.2	20.0
120	0.86	28.0	80.4	19.4
140	0.85	27.8	79.1	18.7

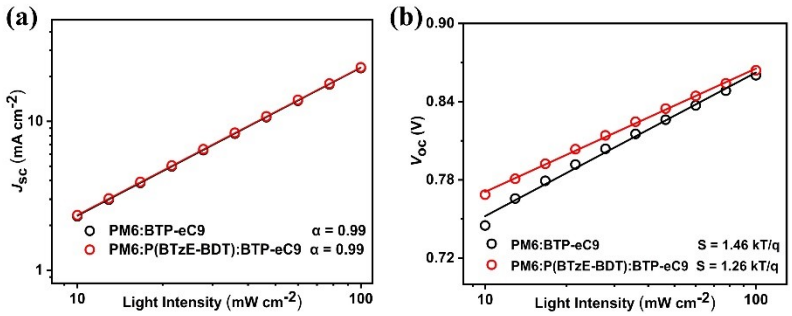

Figure S18. light intensity versus (a) J_{SC} and V_{OC} (b) of binary and ternary organic solar cells.

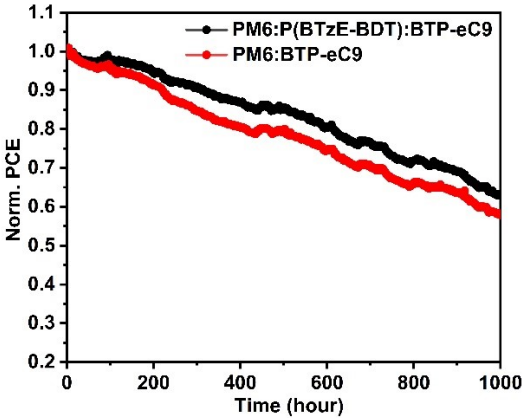

Figure S19. The long-term photostability of the PM6:BTP-eC9 and PM6:P(BTzE-BDT):BTP-eC9 devices

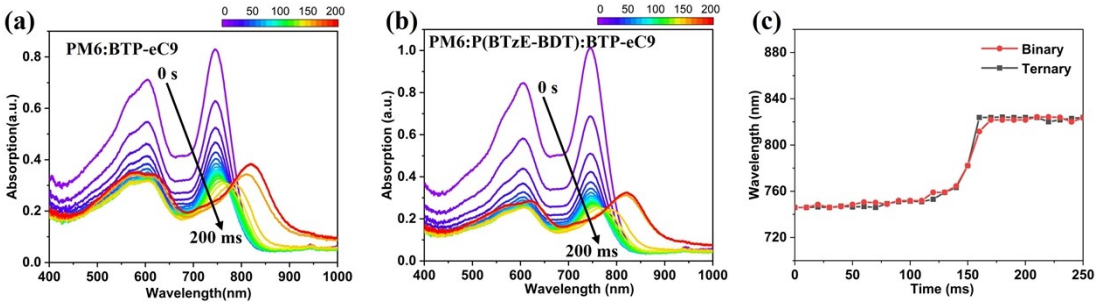

Figure S20. *In-situ* UV-vis absorption spectra of the (a) PM6:BTP-eC9 and (b) PM6:P(BTzE-BDT):BTP-eC9 during the film-drying process. (c) Time evolution of the BTP-eC9 peak location extracted from the corresponding absorption contour map, showing the phase transition.

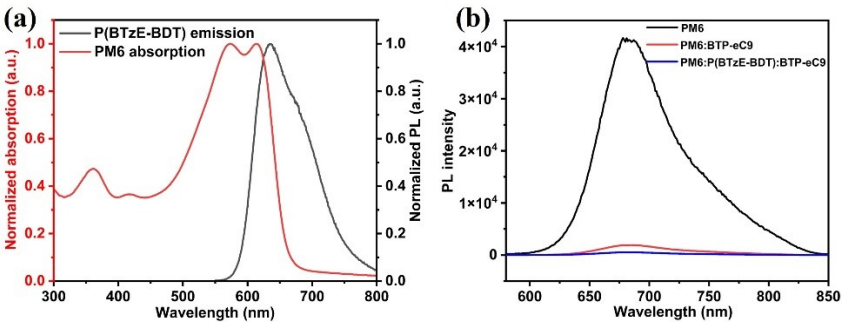

Figure S21. (a) Absorption spectra of PM6 and PL emission spectra of P(BTzE-BDT); (b) PL spectra of the PM6, PM6:BTP-eC9 and PM6:P(BTzE-BDT):BTP-eC9 blend films.

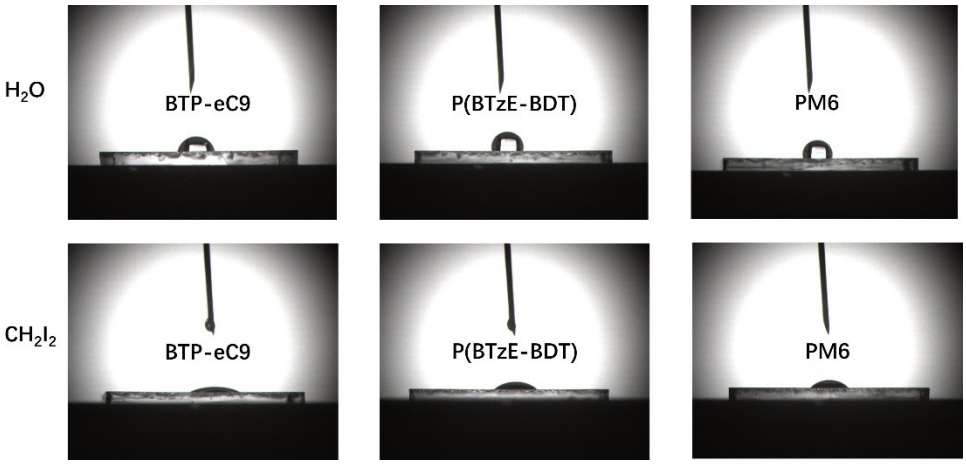

Figure S22. Contact angle images of neat BTP-eC9, P(BTzE-BDT), and PM6 films with water and diiodomethane droplet on top.

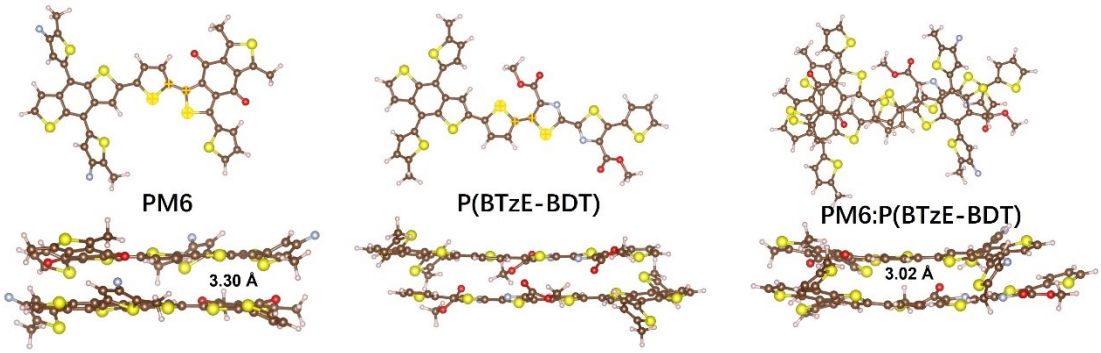

Figure S23. Optimized molecular conformations of the three D/D pairs.

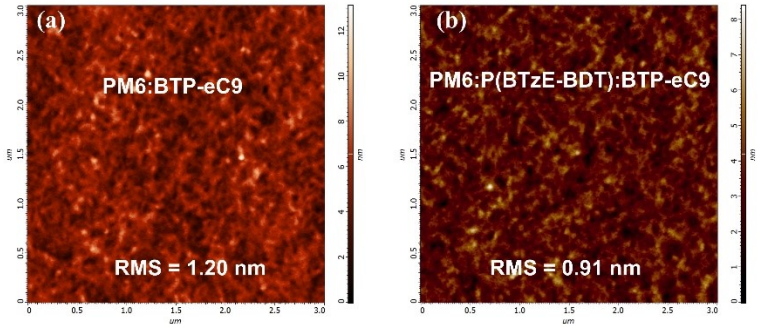

Figure S24. Morphology characterization of the binary (a) and (b) ternary blend films.

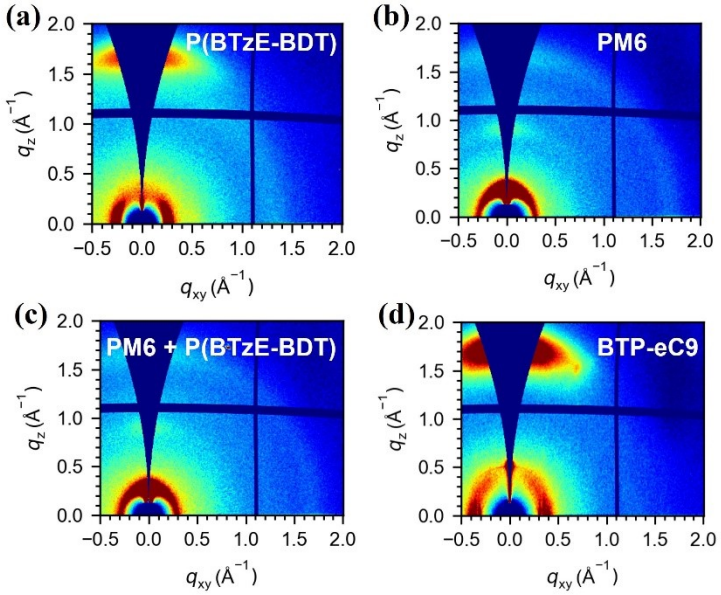

Figure S25. 2D GIWAXS patterns of (a-d) P(BTzE-BDT), PM6, PM6:P(BTzE-BDT) and BTP-eC9 films.

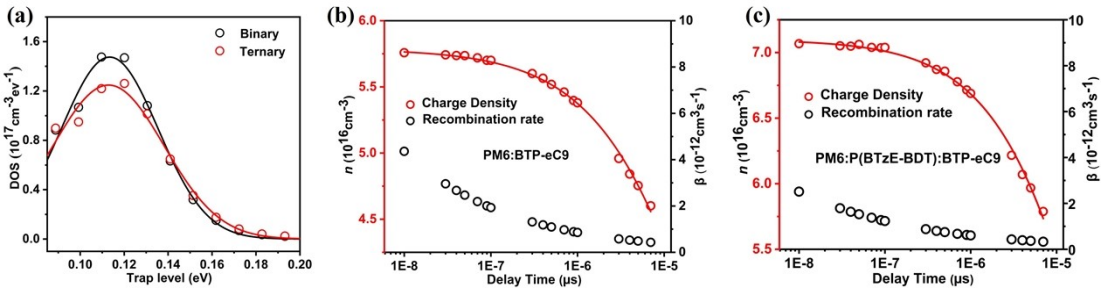

Figure S26. (a) The trap DOS curve of PM6:BTP-eC9 and PM6:P(BTzE-BDT):BTP-eC9 thick films device. The charge carrier density as a function of the delay time of the PM6:BTP-eC9 (b) and (c) PM6:P(BTzE-BDT):BTP-eC9 thick films devices.

References

1. Peng, X. Cao, Y. Jen, A. K. Y. *Adv. Funct. Mater*., 2020**, 30**, 1909535.
2. Chen, C. Wang, L. Sun, Y. Fu, Y. Guo, C. Zhou, B. Gan, Z. Liu, D. Li, W. Wang, T. *Adv. Funct. Mater*., 2023**, 33**, 2305765.
3. Wei, Y. Cai, Y. Gu, X. Yao, G. Fu, Z. Zhu, Y. Yang, J. Dai, J. Zhang, J. Zhang, X. Hao, X. Lu, G.; Tang, Z. Peng, Q. Zhang, C. Huang, H. *Adv. Mater.* 2023**, 36**, 2304225.
4. Ye, Q. Chen, Z. Yang, D. Song, W. Zhu, J. Yang, S. Ge, J. Chen, F. Ge, Z. *Adv. Mater.*, 2023**, 35**, 2305562.
5. Liu, X. Zhang, Z. Wang, C. Zhang, C. Liang, S. Fang, H. Wang, B. Tang, Z. Xiao, C. Li, W., *Angew. Chem., Int. Ed.*, 2023, **63,** e202316039.
6. G. S. Xie, Z. L. Zhang, Z. Y. Su, X. L. Zhang, J. Zhang, *Nano. Energy.* 2020, **69**, 104447.
7. X. P. Xu, K. Feng, Y. W. Lee, H. Y. Woo, G. J. Zhang, Q. Peng, *Adv. Mater*., 2020, **30**, 1907570.
8. J. H. Han, X. C. Wang, D. Huang, C. M. Yang, R. Q. Yang, X. C. Bao, *Macromolecules.*, 2020, **53**, 6619.
9. B. H. Jiang, Y. P. Wang, C. Y. Liao, Y. M. Chang, Y. W. Su, R. J. Jeng, C. P. Chen, *ACS Appl. Mater. Interfaces.,* 2021, **13**, 1076.
10. J. X. Wang, C. Y. Han, F. Z. Bi, D. Huang, Y. W. Wu, Y. H. Li, S. G. Wen, L. L. Han, C. M. Yang, X. C. Bao, J. H. Chu, *Energy Environ. Sci*., 2021, **14**, 5968.
11. Q. S. An, J. W. Wang, X. L. Ma, J. H. Gao, Z. H. Hu, B. Liu, H. L. Sun, X. G. Guo, X. L. Zhang, F. J. Zhang, *Energy Environ. Sci*., 2020, **13**, 5039.
12. H. Xia, Y. Zhang, W. Y. Deng, K. Liu, X. X. Xia, C. J. Su, U. S. Jeng, M. Zhang, J. M. Huang, J. W. Huang, C. Q. Yan, W. Y. Wong, X. H. Lu, W. G. Zhu, G. Li, *Adv. Mater*., 2022, **34**, 2205638.
13. W. T. Zou, C. Y. Han, X. Zhang, J. W. Qiao, J. F. Yu, H. J. Xu, H. H. Gao, Y. N. Sun, Y. Y. Kan, X. T. Hao, G. H. Lu, Y. G. Yang, K. Gao, *Adv. Energy. Mater*., 2023, **13**. 2300784.
14. R. J. Ma, C. Q. Yan, J. S. Yu, T. Liu, H. Liu, Y. H. Li, J. Chen, Z. H. Luo, B. Tang, X. H. Lu, G. Li, H. Yan, *ACS Energy Lett*., 2022, **7**, 2547.
15. L. Zhu, M. Zhang, J. Q. Xu, C. Li, J. Yan, G. Q. Zhou, W. K. Zhong, T. Y. Hao, J. L. Song, X. N. Xue, Z. C. Zhou, R. Zeng, H. M. Zhu, C. C. Chen, R. C. I. MacKenzie, Y. C. Zou, J. Nelson, Y. M. Zhang, Y. M. Sun, F. Liu, *Nat. Mater.*, 2022, **21**, 656.
16. Liu, S. Wang, J. Wen, S. Bi, F. Zhu, Q.Yang, C.; Yang, C. Chu, J. Bao, X. *Adv. Mater*., 2024, **36**, 2312959.
17. Zhang, W. Huang, J. Xu, J.; Han, M. Su, D. Wu, N. Zhang, C. Xu, A. Zhan, C. *Adv. Energy. Mater*., ***2020***, **10**, 2001436.